# Mitochondrial Aconitase Modification, Functional Inhibition, and Evidence for a Supramolecular Complex of the TCA Cycle by the Renal Toxicant *S*-(1,1,2,2-Tetrafluoroethyl)-L-cysteine†

Eric A. James,‡ Steven P. Gygi,§ Michael L. Adams,‡ Robert H. Pierce,|| Nelson Fausto,⊥ Ruedi H. Aebersold,# Sidney D. Nelson,‡ and Sam A. Bruschi*,‡

*Departments of Medicinal Chemistry and Pathology, University of Washington, Seattle, Washington 98195, Department of Cell Biology, Harvard Medical School, Boston, Massachusetts 02115, Department of Pathology and Laboratory Medicine, University of Rochester School of Medicine and Dentistry, Rochester, New York 14642, and The Institute for Systems Biology, 4225 Roosevelt Way, Suite 200, Seattle, Washington 98105-6099*

*Received January 15, 2002*

ABSTRACT: Metabolism of the common industrial gas tetrafluoroethylene in mammals results in the formation of *S*-(1,1,2,2)-tetrafluoroethyl-L-cysteine (TFEC), which can be bioactivated by a mitochondrial C-S lyase commonly referred to as *β*-lyase. The resultant "reactive intermediate", difluorothioacetyl fluoride (DFTAF), is a potent thioalkylating and protein-modifying species. Previously, we have identified mitochondrial HSP70, HSP60, aspartate aminotransferase, and the E2 and E3 subunits of the α-ketoglutarate dehydrogenase (αKGDH) complex as specific proteins structurally modified during this process. Moreover, functional alterations to the αKGDH complex were also detected and implicated in the progression of injury. We report here the identification, by tandem mass spectrometry, and functional characterization of the final remaining major protein species modified by DFTAF, previously designated as P99(unk), as mitochondrial aconitase. Aconitase activity was maximally inhibited by 56.5% in renal homogenates after a 6 h exposure to TFEC. In comparison to αKGDH, aconitase inhibition (up to 79%) in a cell culture model for TFEC-mediated cytotoxicity was greater and preceded αKGDH inhibition, indicating that aconitase modification may constitute an early event in TFEC-mediated mitochondrial damage and cell death. These findings largely define the initial lesion of TFEC-mediated cell death and also have implications for the modeling of mitochondrial enzymatic architecture and the localization and identity of renal mitochondrial cysteine S-conjugate *β*-lyase.

The mechanism of cell death and organ damage produced by *S*-(1,1,2,2)-tetrafluoroethyl-L-cysteine (TFEC)[1] is expected to follow the "covalent binding hypothesis" whereby the covalent modification of critical proteins by reactive intermediates of metabolism results in a functional deficit of the target protein(s) and subsequent pathology (*1*, *2*).

In contrast to other intensively studied examples of such "covalent binding"-mediated injury, e.g., acetaminophen (*3*) and halothane (*4*), the identification of TFEC-modified proteins has provided valuable insight into the mechanism by which TFEC causes cell death. This is primarily due to the relative simplicity and site selectivity of the proteins modified. For example, our previous studies have indicated that only mitochondrial proteins are targeted, and these are limited to HSP60, HSP70, aspartate aminotransferase (AAT), and the lipoamide succinyltransferase (E2o) and dihydrolipoamide dehydrogenase (E3o) subunits of the αKGDH complex (*5*, *6*). The identity of these target proteins is consistent with the known site-selective specificity of TFEC-mediated damage to mitochondria of the mammalian renal proximal tubular epithelium (*5*).

The metabolism of tetrafluoroethylene proceeds through sequential glutathione *S*-transferase, *γ*-glutamyl transpeptidase, and cysteinylglycine dipeptidase activities to produce the corresponding cysteine conjugate, TFEC (*7*). Although this is generally a detoxification pathway, TFEC may also become activated in the renal proximal tubular epithelium to an unstable α-fluorothiolate, tetrafluoroethanethiolate, by a cysteine S-conjugate *β*-lyase of uncertain identity. Collapse of the thiolate yields a transient, but potent, acylating species, 2,2-difluorothioacetyl fluoride (DFTAF), which covalently modifies lysyl *ε*-amino groups of neighboring proteins to produce difluorothioamidyl-L-lysine moieties (DFTAL, ref *7*, Figure 1).

† This work was supported by NIH Grants GM51916 to S.A.B., GM25418 to S.D.N., R01 A1 41109-01 and RR11823 to R.H.A., and CA74131 to N.F. and by NIEHS Center Grant P30 ES07033.

* To whom correspondence should be addressed. Telephone: (206) 543-7360. Fax: (206) 685-3252. E-mail: sambru@u.washington.edu.

‡ Department of Medicinal Chemistry, University of Washington.

§ Harvard Medical School.

|| University of Rochester School of Medicine and Dentistry.

⊥ Department of Pathology, University of Washington.

# The Institute for Systems Biology.

[1] Abbreviations: AAT, mitochondrial isoform of aspartate aminotransferase; BA, bongkrekic acid; DFTAF, difluorothioacetyl fluoride; DFTAL, difluorothioamidyl-L-lysine; E2o, lipoamide succinyltransferase subunit of α-ketoglutarate dehydrogenase complex; E3o, dihydrolipoamide dehydrogenase subunit of α-ketoglutarate dehydrogenase complex; HSP60, mitochondrial stress protein, 60 kDa; HSP70, mitochondrial stress protein, 70 kDa; αKGDH, α-ketoglutarate dehydrogenase complex; TFEC, *S*-(1,1,2,2-tetrafluoroethyl)-L-cysteine.

10.1021/bi020038j CCC: $22.00 © 2002 American Chemical Society
Published on Web 05/02/2002

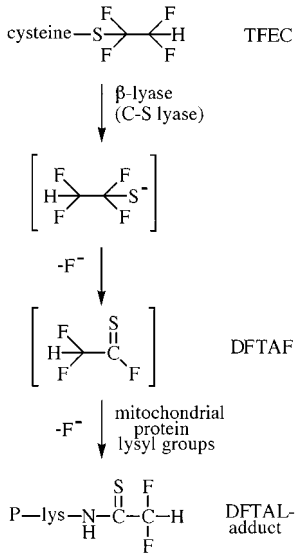


FIGURE 1: Mitochondrial bioactivation of TFEC. A $\beta$-lyase (C-S lyase) activity located within mammalian mitochondria is proposed to result in conversion of tetrafluoroethylcysteine (TFEC) to tetrafluoroethanethiolate with subsequent rearrangement to difluoroacetyl fluoride (DFTAF) and, ultimately, covalent alteration of mitochondrial proteins at lysine residues (DFTAL-adduct). Direct observation of the reactive intermediates shown in square brackets has not been observed but is favored from indirect evidence (refer text).

Using both immunochemical and radiochemical techniques five major DFTAL-containing proteins have been detected in a rodent model of TFEC-induced renal damage (*5*, *6*). In previously reported studies we have identified four of the five major protein targets, and these can be subdivided into two categories; viz., (1) enzymes of intermediary metabolism associated with the TCA cycle ($\alpha$KGDH complex, AAT) and (2) mitochondrial stress proteins (HSP60 and HSP70). Subsequent work has indicated that DFTAF-mediated adduction of mitochondrial stress proteins likely represents a secondary event to the modification of TCA cycle enzymes as HSP60 and HSP70 mobilize in response to the primary lesion (*5*).

To more completely define the mechanism of TFEC-mediated cell death, we have partially purified, identified, and functionally characterized the final remaining major protein target of TFEC. Our data indicate that this ≈99 kDa protein is mitochondrial aconitase and that inhibition of renal aconitase activity both in vivo and in vitro is a functional consequence of difluorothioamidyl-L-lysine formation by TFEC. In addition, the labile characteristics of the TFEC-reactive metabolite provides further in situ information regarding TFEC-mediated cell death and mitochondrial biochemistry/physiology.

## EXPERIMENTAL PROCEDURES

*TFEC Synthesis.* TFEC was synthesized as previously reported (*5*) using tetrafluoroethylene (SynQuest Laboratories Inc., Alachua, FL) and L-cysteine (Sigma, St. Louis, MO). Mass spectrometry (Micromass Quattro II, Manchester, U.K.) and nuclear magnetic resonance (Varian Associates VXR 300, Palo Alto, CA) were used to confirm product identity and purity.

*Dosing and Tissue Collection.* Male Fischer 344 rats weighing 200−250 g (Charles River Laboratories, Wilmington, MA) were acclimatized for 2 weeks at the University of Washington in an IACUC-approved facility prior to dosing. Rats received either 30 mg/kg (ip) TFEC ($n = 25$) or the corresponding vehicle (PBS, $n = 28$). After 6, 12, and 24 h animals were euthanized, and kidneys were removed immediately, decapsulated, rinsed in normal saline, flash frozen in liquid nitrogen, and stored at −80 °C for subsequent analyses.

*Immunoblot Detection of DFTAL-Modified Proteins from Renal Homogenates.* Kidneys from TFEC-treated and vehicle-injected control animals were homogenized in a Tris buffer (20 mM Tris, 250 mM sucrose, 5 mM EDTA, 10 $\mu$g/mL antipain, 10 $\mu$g/mL aprotinin, 10 $\mu$g/mL leupeptin, and 1 mM dithiothreitol, pH 7.4; volume equal to 10 times tissue weight). Total protein content was determined using the Bradford assay (Bio-Rad Laboratories, Hercules, CA). Tissue homogenate proteins were separated by denaturing gel electrophoresis (Mini-PROTEAN II, Bio-Rad) using 8% gels and 50 $\mu$g of total protein per lane. Prestained broad-range molecular mass standards were run concurrently (New England Biolabs, Inc., Beverly, MA). Resolved proteins were transferred to a nitrocellulose membrane using a semidry transfer apparatus (Bio-Rad) and probed with an anti-difluorothioamidyl-L-lysine ($\alpha$DFTAL) antibody [1:2000 in PBS, 0.1% Tween 20 (v/v), 4% nonfat dried milk (w/v), pH 7.4; Dr. L. Pohl, NIH]. Immunoreactive proteins were detected with enhanced chemiluminescence using Super-Signal West Dura substrate (Pierce Chemical Co., Rockford, IL).

*Partial Purification of P99 by DEAE Anion-Exchange Chromatography.* Whole kidney tissue homogenized in HEPES buffer (2 mM HEPES, 70 mM sucrose, 220 mM mannitol, 0.1% CHAPS, 1.0 mM EDTA, 5 $\mu$g/mL antipain, 2 $\mu$g/mL aprotinin, and 5 $\mu$g/mL leupeptin, pH 7.4) was centrifuged at 1000*g* for 10 min. The supernatant was centrifuged at 10000*g* for 15 min, and the resultant supernatant was discarded. The new pellet was washed and resuspended in homogenization buffer and centrifuged at 10000*g* for 15 min. Mitochondrial proteins were solubilized at 0 °C in TEDC buffer [20 mM Tris, 0.1 mM EDTA, 2 mM dithiothreitol, 1% (w/v) CHAPS, pH 7.4] and centrifuged for 40 min at 100000*g* prior to anion-exchange chromatography of the supernatant. A 2 × 20 cm DEAE-Sepharose (Sigma) chromatography column (Amersham Pharmacia Biotech, Piscataway, NJ) was equilibrated to 4 °C with 20 mM Tris, 0.1 mM EDTA, 2 mM dithiothreitol, and 0.1% CHAPS, pH 7.4, and loaded mitochondrial proteins were eluted in 6 mL fractions ($n = 100$) using a linear NaCl gradient (0.0−0.7 M).

*SDS−PAGE Purification of P99.* An aliquot from every third chromatography fraction was subjected to SDS−PAGE using 8% gels as described above. Resolved proteins were visualized by silver staining according to a protocol adapted from Shevchenko et al. (*8*). Fractions containing a protein with an apparent molecular mass of 99 kDa were concentrated by size exclusion centrifugation (Microcon, Millipore Corp., Bedford, MA) at 12000*g* for 20 min. Concentrated fractions were pooled, assayed for total protein content, and confirmed as containing difluorothioamidyl-L-lysine modifications by immunoblot with $\alpha$DFTAL antiserum as described above.

*In-Gel Tryptic Digestion of P99.* Fractions containing P99 were pooled, concentrated by size exclusion centrifugation (Microcon, Millipore Corp.), and purified by further SDS−PAGE as described above. Multiple lanes of approximately 15 $\mu$g of total protein were run, silver stained, and dried overnight between cellulose sheets (Promega Corp., Madison, WI). Three silver-stained bands, each containing approximately 100 ng of P99, were excised and subjected to in-gel tryptic digestion (*8*). Cellulose-encased bands were placed in a siliconized microcentrifuge tube (Costar, Corning Inc., Corning, NY) and rehydrated with Nanopure water (Millipore). Cellulose pieces were discarded, and the gel bands were destained with 30 mM potassium ferricyanide and 100 mM sodium thiosulfate, washed, dehydrated with 100% acetonitrile, and dried by vacuum centrifugation. Gel pieces were incubated for 1 h at 0 °C in a solution containing 12.5 ng/mL modified porcine trypsin (Promega, V511C, Madison, WI), 50 mM ammonium bicarbonate, and 5 mM calcium chloride. Excess trypsin solution was removed and replaced with 10 $\mu$L of a trypsin-free solution of 50 mM ammonium bicarbonate and 5 mM calcium chloride. The preparation was incubated overnight at 37 °C. Tryptic peptides were then extracted by incubating the gel pieces for 20 min in 20 mM ammonium bicarbonate solution. Supernatants were pooled, and the remaining peptides were eluted from the gel matrix with three 20 min washes of 50% (v/v) acetonitrile and 5% (v/v) formic acid. All supernatants from the preceding steps were pooled. The final solution of tryptic peptides was dried by vacuum centrifugation, reconstituted in 10 $\mu$L of 0.3% (v/v) trifluoroacetic acid, and desalted on a C18-silica-filled pipet tip (ZipTip, Millipore).

*Identification of P99 by LC-MS/MS.* Utilizing the techniques described by Yates et al. (*9*) and Gygi et al. (*10*), tryptic peptides from P99 were characterized by tandem mass spectrometry. Briefly, tryptic peptides were separated online by microcapillary liquid chromatography prior to introduction into a TSQ 7000 triple quadrupole mass spectrometer (Finnigan, San Jose, CA). LC-MS-detected peptides of sufficient abundance were analyzed by collision-induced dissociation via automated switching to MS/MS mode (for peptide sequencing and characterization). Peptide fragmentation spectra were searched against the OWL Composite Protein Sequence Database (version 30.3) using Sequest software (*11*, *12*), which correlates theoretical and acquired MS/MS spectra. Unambiguous protein identification was attained in a single analysis by the detection of multiple peptides derived from the same protein.

*Cell Culture Conditions.* The serum-free culture of the TAMH line, passages 19−35, was as previously described (*13*). Briefly, growth and passage of cells were in serum-free Dulbecco's modified Eagle's medium/Ham's F12 (Gibco, Rockville, MD) supplemented with insulin, transferrin, selenium (Collaborative Biomedical Products, Bedford, MA), dexamethasone, nicotinamide, and gentamycin. Cultures were maintained in a humidified incubator with 5% carbon dioxide/95% air atmosphere and passaged when 70−90% confluent (approximately 5−7 days).

*Cell Viability Determinations.* Cellular viability was assessed by the Live/Dead Cytotoxicity Kit (Molecular Probes, Eugene, OR), based on intracellular esterase formation of calcein from cell-permeant calcein acetoxymethyl ester or nuclear entry of impermeant ethidium homodimer. Assay procedures were conducted exactly as described by the manufacturer.

*Gel Electrophoresis.* Protein samples (50 $\mu$g per lane) were resolved on 10% SDS−PAGE minigels (Mini-Protean, II, Bio-Rad, Hercules, CA) and transferred to nitrocellulose (1 h, 15 V, Trans-Blot SD Semi-Dry Transfer Cell, Bio-Rad). Immunodetection was by chemiluminescence (SuperSignal ULTRA, Pierce, Rockford, IL) using antibodies specific for the DFTAL protein adduct (Dr. L. Pohl, NIH).

*Measurement of Aconitase Activity.* Aconitase activity was measured spectrophotometrically by monitoring the depletion of *cis*-aconitate (Sigma) as previously described (*14*). Briefly, total renal tissue homogenates or TAMH cell lysates were prepared after TFEC or vehicle treatment by homogenization in 50 mM Tris (pH 8.2), 5 mM $MgCl_2$, and 1 mM EDTA. Aliquots of the homogenates were stored at −80 °C for subsequent analysis. Assay volumes (20 $\mu$L) were added to a 1 mL quartz cuvette containing 0.9 mL of assay buffer [22 mM Tris−acetate, 220 mM NaCl, 0.33 mM *cis*-aconitate (Sigma, A3412), pH 7.2] with changes in absorbance at 240 nm monitored over 5 min. Aconitase activity was calculated using the extinction coefficient of 3.7 $M^{-1}\cdot cm^{-1}$. Differences in TFEC-treated and control substrate consumption plots were assessed for statistical significance using a two-sample pooled *t*-test for comparison of means.

*Electron Microscopy.* Adherent and nonadherent cells from 250 $\mu$M TFEC-treated and saline vehicle control TAMH cultures were fixed using Karnovsky's fixative (one-half strength glutaraldehye−formaldehyde), washed with two changes of Sorensen's phosphate buffer, and stained for 15 min in 1.0% osmium tetroxide (in Sorensen's phosphate buffer). Cells were dehydrated in a graded ethanol series up to 100% and embedded with epoxy resin. Ultrathin sections were cut with a diamond knife on a LKB NOVA ultramicrotome, placed onto copper grids, and stained with 2.0% aqueous uranyl acetate and Reynold's lead citrate. A Hitachi 7100 electron microscope was used to examine and photograph samples.

## RESULTS

Previous attempts to identify DFTAL-modified P99 (DFTAL-P99) using Edman degradation were unsuccessful, indicating that this protein was most likely blocked at the amino terminus. Consequently, an alternative strategy was employed. DFTAL-P99 was partially purified from total renal tissue homogenate prepared 6 h after treatment with a nonlethal dose of TFEC (30 mg/kg ip) using differential centrifugation and DEAE-Sepharose anion-exchange chromatography (Figure 2A). A major ≈99 kDa protein was detected by silver staining in early column and flow-through fractions only (Figure 2B). These column fractions were pooled, and DFTAL chemical modification was confirmed by immunoblot analyses after further spin column concentration (Figure 2C). The major αDFTAL immunoreactive protein at approximately 99 kDa was then digested with trypsin and desalted, and primary sequence information was derived by tandem mass spectrometry.

DFTAL-P99 identity was determined by automated correlation of tandem mass spectrometry-derived primary sequence fragmentation data (Figure 3A) with theoretical fragmentation patterns from sequence databases (*10*, *12*). A

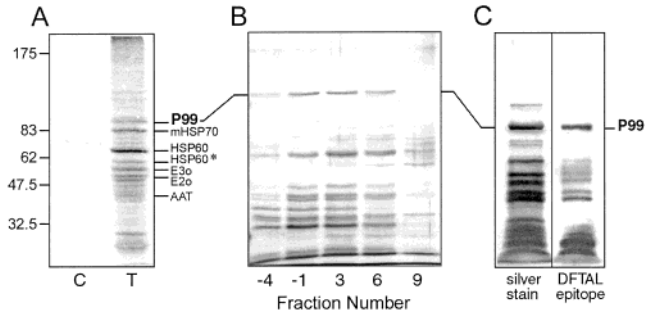


FIGURE 2: Partial purification of DFTAL-modified P99. Rat kidney tissue homogenate prepared 6 h after saline vehicle (C) or 30 mg/kg (ip) TFEC treatment (T) was immunoblotted to confirm the presence of DFTAL-modified proteins (A). TFEC-treated mitochondria were then isolated by differential centrifugation and subjected to DEAE-Sepharose anion-exchange chromatography, denaturing PAGE, and silver staining to locate the predominant ≈99 kDa protein (B). Pooled fractions containing P99 were concentrated, silver-stained (C, left panel), and immunoblotted with αDFTAL-specific antisera (C, right panel) to confirm DFTAL modification prior to further isolation with SDS−PAGE, tryptic digestion, and tandem mass spectrometry. The identities of major DFTAL-adducted proteins are indicated on the right of panel A in addition to the relative migration of P99. HSP60* represents the major 56 kDa proteolytic fragment of HSP60 as identified by N-terminal sequencing (data not presented). Molecular mass standard mobilities are shown only on the left of panel A for clarity.

total of 13 peptide fragments were matched to bovine aconitase. Of these, 9 peptides had cross-correlation scores indicative of a high match probability (Figure 3B; >3 indicative of excellent correlation). Although a rodent aconitase sequence was not present in the databases at the time of searching, subsequent submission of a mitochondrial aconitase sequence from *Rattus norvegicus* confirmed the extensive identity between the two homologues [96% overall identity between bovine (Accession Number S57528) and rat (Accession Number CAC11018), with 7 of 9 high correlation fragments from Figure 3B being 100% identical between the two species].

The functional consequence of DFTAL modification on mitochondrial aconitase was assessed by determining aconitase enzymatic activity at various times after treatment with TFEC both in vivo and in vitro (Table 1, Figure 4). Aconitase activity in vivo was significantly inhibited at all time points examined after TFEC treatment with a maximal inhibition of 56.5% at 6 h ($p \ll 0.001$, Table 1). Some recovery was evident at 12 and 24 h following treatment although significantly still lowered in comparison to control treatments (39.4%, $p < 0.005$, and 31.5%, $p < 0.05$, respectively). These alterations to in vivo aconitase activities are in keeping with an expected alteration to function after DFTAL modification. In comparison to our previous studies, which indicated maximal inhibition of the αKGDH complex at 12 h (*5*), these data indicate comparative in vivo inhibitions of mitochondrial aconitase activity much earlier after TFEC administration.

To begin to address the functional significance of TFEC-mediated aconitase inhibition, studies were undertaken using the TAMH cell line (*13*). Morphologically, dose-related cell lifting from monolayer cultures was observed even at low micromolar doses of TFEC (100−200 μM, Figure 4A). Quantitative analyses of cell viability confirmed that TFEC-induced cell lifting was equivalent to cell death (Figure 4B) and that DFTAL formation on proteins accompanied loss of viability in vitro (Figure 4C). Although the identities of DFTAL-modified proteins produced in the TAMH line have not yet been established, a good agreement with in vivo identities appeared to be evident, based on molecular mass calculations. Addition of the proteasome-directed inhibitor MG132 was also observed to increase DFTAL−protein formation in vitro (Figure 4C). Furthermore, examination of the activities of both aconitase and αKGDH targets in TAMH cultures indicated TFEC-directed inhibition in a dose-related manner consistent with our in vivo findings (Figure 4D).

The morphologies of TAMH cells were also examined using electron microscopy at early intervals after TFEC treatment (Figure 5A). Mitochondria were structurally altered at both 2 and 4 h after TFEC treatment with swelling of the matrix evident, which resulted in large, cristae-deficient areas (Figure 5A). Although not assessed quantitatively, the incidence of altered mitochondria appeared higher at 4 h in comparison to 2 h. These changes to mitochondrial morphology, even though reminiscent of a permeability transition phenomenon, were not associated with activation of caspase 6, 9, 3, or 7 as determined by cleavage of fluorometric tetrapeptide substrates (data not presented). Nonetheless, the permeability transition inhibitor bongkrekic acid effectively inhibited cell death over an extended period of time after exposure to low (100 μM) and, to a lesser extent, very high concentrations (250 μM) of TFEC (Figure 5B).

## DISCUSSION

Considerable evidence from many different organisms indicates that mitochondrial aconitase activity is uniquely sensitive to various physiological and pathological conditions. For example, inhibition of the mitochondrial isoform occurs with peroxynitrite, nitric oxide, and excessive superoxide formation during oxidative stress (*14*−*18*). Inborn errors of metabolism have also been found which either directly (*19*) or indirectly (*20*) inhibit mitochondrial aconitase activity. Although still contentious, the protein product associated with Friedreich ataxia, frataxin, is believed to alter aconitase activity via mitochondrial Fe utilization (*20*). In comparison, a single report of direct aconitase deficiency coupled with defects in succinate dehydrogenase (*19*) implicates problems with Fe/S cluster assembly and/or synthesis in this inherited disorder (refer later). Our data indicate that aconitase is also a target during TFEC-mediated cell death despite previous work indicating no evidence for an oxidative stress component (*21*) and, to the best of our knowledge, represent the first example of a man-made chemical covalently targeting this protein. As a result TFEC-mediated cell death resembles, in part, damage by purely oxidative stresses and aging (*15*, *16*, *22*).

In addition, our in vitro data indicated that aconitase inhibition is likely to play an important part in TFEC-mediated cytotoxicity based on an earlier and greater level of inhibition of this enzyme in comparison to αKGDH complex inhibitory effects (Figure 4). Matrix swelling of mitochondria was also observed in response to TFEC treatment of TAMH cultures, suggesting that a downstream permeability transition is mechanistically coupled to aconitase and/or αKGDH inhibition. In support of this we have found that BA, a specific inhibitor of the mitochondrial permeability transition pore component, the inner membrane ADP/ATP

A

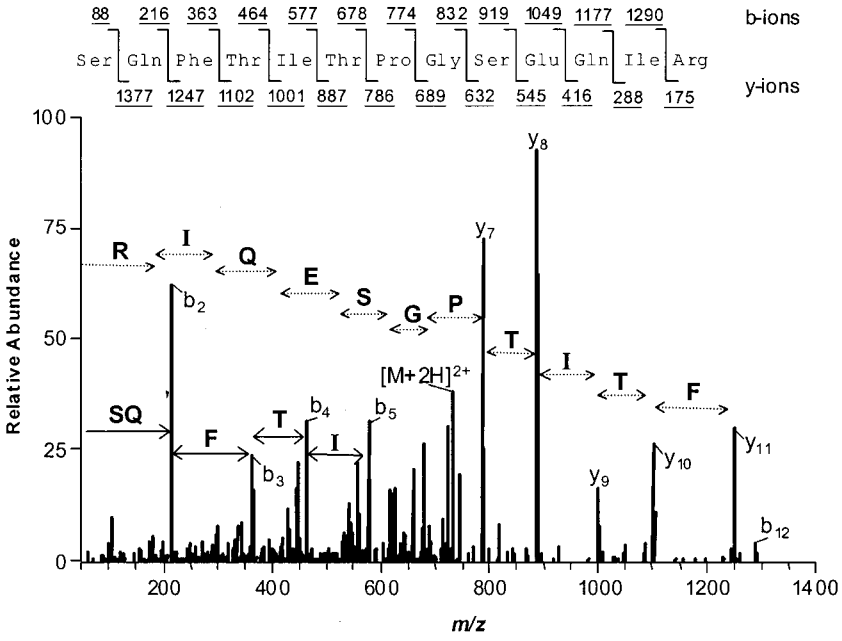


B

| Ion Mass | Sequence | Cross-Correlation |
|---|---|---|
| 1869.6 | (K)IVYGHLDDPANQEIER | 5.9647 |
| 799.7 | (K)VAGLLTVK | 2.8344 |
| 985.5 | (K)EGWPLDIR | 3.0976 |
| 1464.0 | (K)SQFTITPGSEQIR | 3.6451 |
| 1268.7 | (K)FNPETDFLTGK | 2.4765 |
| 1502.0 | (K)FKLEAPDADELPR | 2.0339 |
| 1732.4 | (R)AEFDPGQDTYQHPPK | 2.2905 |
| 1800.0 | (R)DLEDLQILIKVK#GK# | 2.4553 |
| 1601.5 | (R)NAVTQEFGPVPDTAR | 4.8135 |

FIGURE 3: Identification of DFTAL-modified P99. (A) Tandem mass (MS/MS) spectrum derived from collision-induced dissociation of the $(M + 2H)^{2+}$ precursor, *m/z* 733. Fragment ions in the spectrum represent mainly single-event preferential cleavage of the peptide bonds resulting in sequence information being recorded simultaneously from both the N and C termini (b- and y-type ions, respectively). This spectrum was computer searched with the Sequest program (*11*) and was matched to the bovine aconitase tryptic peptide shown. The spectrum is representative of 12 other peptides that were also identified as being derived from aconitase. (B) Nine tryptic peptides from rat renal DFTAL-P99 identified by LC-MS/MS yielded high cross-correlation scores by Sequest with nine theoretical tryptic fragments from bovine aconitase (Accession Number S57528). A # denotes a modified lysine (K) residue.

Table 1: Confirmation of DFTAL-Mediated Inhibition of *cis*-Aconitate Metabolism in Rat Renal Homogenates after TFEC Treatment (30 mg/kg ip)

| treatment | time (h) | aconitase activity ($\mu$mol of *cis*-aconitate turnover $mg^{-1}$ $min^{-1}$) | SD (*n*) | inhibition (%) | significance |
|---|---|---|---|---|---|
| control | 0 | 28.26 | 4.4 (7) | | |
| control | 6 | 30.34 | 5.7 (9) | | |
| TFEC | 6 | 13.20 | 5.7 (13) | 56.5 | $p \ll 0.001$ |
| control | 12 | 31.54 | 7.1 (8) | | |
| TFEC | 12 | 19.11 | 7.6 (8) | 39.4 | $p < 0.005$ |
| control | 24 | 31.55 | 5.1 (4) | | |
| TFEC | 24 | 21.60 | 4.7 (4) | 31.5 | $p < 0.05$ |

translocase (*23*), effectively inhibited TFEC-induced necrotic death even over an extended period of time (Figure 5B). Further studies are in progress to address the exact contributions of target protein DFTAL formation and aconitase inhibition in TFEC-induced TAMH cell death.

A well-accepted scheme for the bioactivation of TFEC is outlined in Figure 1. TFEC bioactivation requires metabolism to a proposed thiolate which may ultimately modify free lysine residues, thereby forming protein−DFTAL adducts (Figure 1). The considerable biological reactivity of this reactive intermediate is indicated by the difficulty in directly observing either a thiolate or a thioacyl fluoride species during TFEC metabolism in vivo or in vitro (*24*, *25*). Nonetheless, the collapsed thiolate (DFTAF) has been trapped with aromatic amines to form the corresponding phenyl or benzyl difluorothioacetamides, providing indirect evidence for the pathway shown in Figure 1 (*7*, *24*). An absence of data regarding the stability of tetrafluoroethanethiolate (DFTAF) or any thiolate derivative in aqueous or biological fluids is evident. More comprehensive analyses with structurally analogous alkyl halide derivatives of carboxylic acids indicate that increasing the electron-withdrawing characteristics of the substituent adds further to the excellent leaving group properties of these compounds in aqueous solution (*26*). Taken together, these data indicate

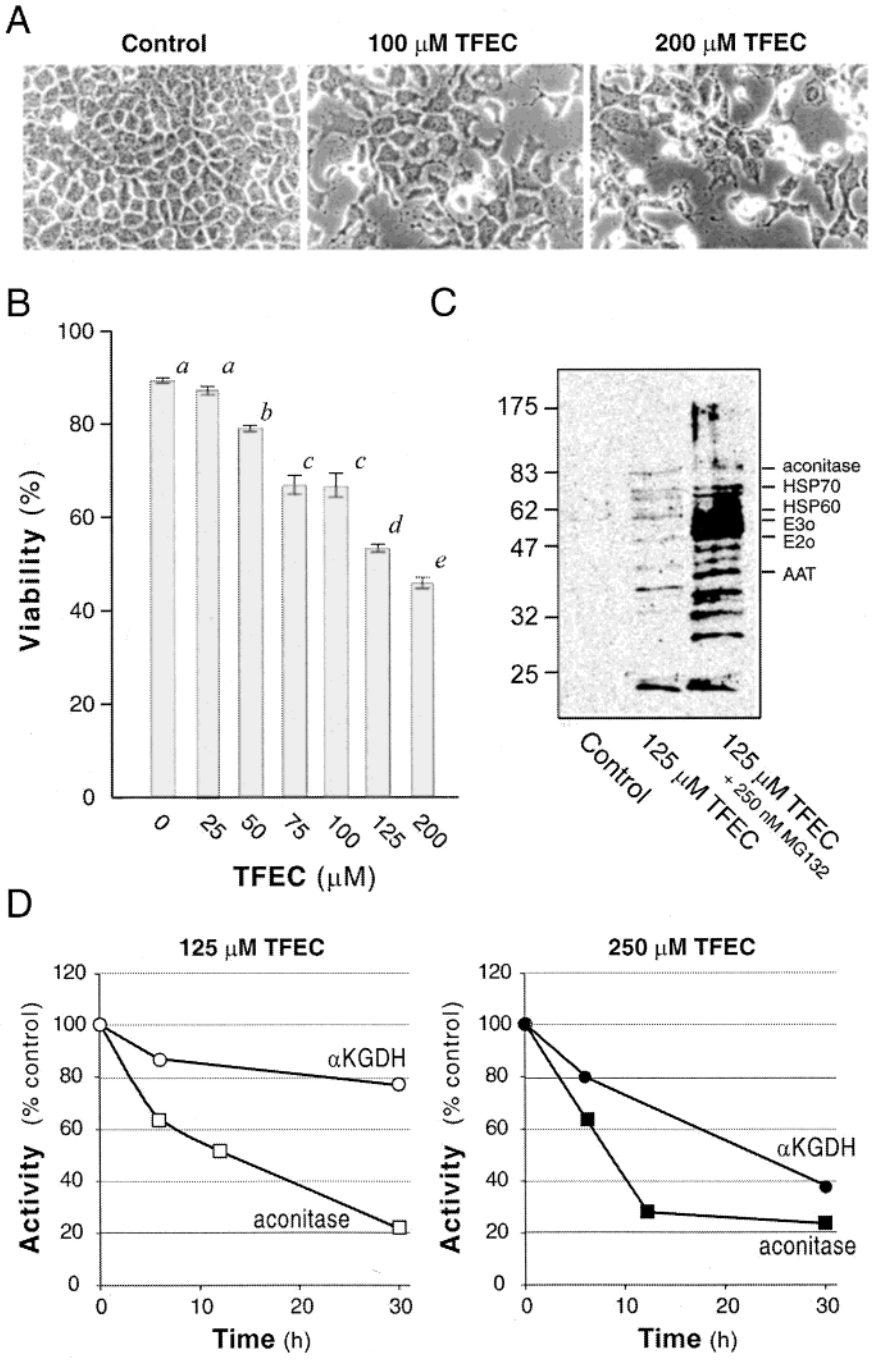


FIGURE 4: Early, dose-related, aconitase inhibition by TFEC precedes cell death in vitro. (A) Cellular morphology by light microscopy of TFEC-induced cytotoxicity in TAMH cultures exposed to saline vehicle (control) or 100 or 200 $\mu$M TFEC for 12 h. Nonadherent and dead cells were observed as smaller, light-colored, spheres out of the plane of focus for all TFEC treatments whereas adjacent healthier cells remained in the culture monolayer (magnification 300×). (B) Quantitative evaluation of cell viabilities in TAMH cultures exposed to TFEC (0−200 $\mu$M) for 12 h. Pooled nonadherent and adherent cells were assessed for viability using Live/Dead assay (refer to Experimental Procedures). Treatments with differing designations were statistically distinct (a−e, $0.05 > p \ll 0.001$). (C) DFTAL−protein formation in vitro after 125 $\mu$M TFEC treatment of TAMH cultures for 12 h as determined by immunoblot using antibody specific to the DFTAL modification (middle, cf. left lane). Addition of the proteasome-directed inhibitor MG132 increased DFTAL adduct formation (right lane). Migration of molecular standards is shown to the left, and the approximate positions of expected protein targets, from in vivo studies, are shown on the right, based on relative mass calculations. (D) Relative time course and extent of aconitase inhibition in vitro with respect to another confirmed TFEC target, the αKGDH complex. Aconitase activities in TAMH cultures ranged from control values of 7.98 $\mu$mol of *cis*-aconitate consumed $min^{-1}$ (mg of protein)$^{-1}$ (±0.0003 $\mu$mol $min^{-1}$ $mg^{-1}$, SD; $n = 3$ independent experiments) to 2.06 $\mu$mol of *cis*-aconitate $min^{-1}$ $mg^{-1}$ in cultures treated with 250 $\mu$M TFEC for 30 h ($n = 2$). αKGDH activities ranged from a maximum of 0.397 $\mu$mol of NADH produced $min^{-1}$ (mg of protein)$^{-1}$ to a minimum of 0.153 $\mu$mol of NADH produced $min^{-1}$ $mg^{-1}$ (values are the average of two independent determinations).

that the reactivity in aqueous solution of thiolates or acyl fluorides is high. Consequently, it is not unreasonable to expect that the half-life in a complex biological fluid, e.g., the mitochondrial matrix, would be even further decreased. With these considerations in mind the identification of DFTAL-modified target proteins will likely reveal novel in situ information on the physical proximity of proteins adjacent to the site of TFEC bioactivation.

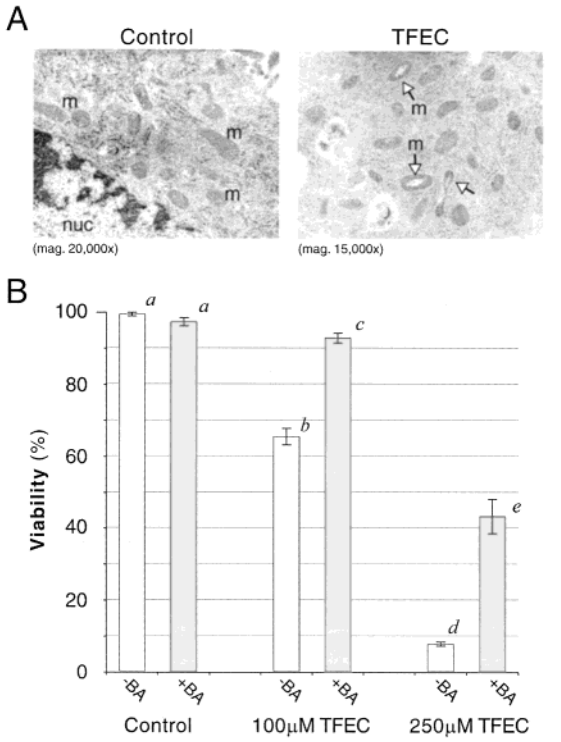


FIGURE 5: Early TFEC-induced alterations to mitochondrial morphology. (A) Examination of TAMH cell morphologies by electron microscopy after treatment with TFEC (250 $\mu$M) or saline vehicle (control) for 4 h. Only TFEC-treated cultures consistently showed the presence of many mitochondria **(**m**)** with matrix swelling as evidenced by enlarged, electron-opaque spaces devoid of cristae (arrows). Morphologically altered mitochondria were also observed in cultures treated for 2 h but were qualitatively less frequent. (B) Inhibition of TFEC-induced cytotoxicity with concurrent 50 $\mu$M bongkrekic acid (BA) treatment at the late time point of 18 h. Data represent mean ± SD from three independent experiments with $n = 3-6$ replicate plates per experiment. Treatments with differing designations were statistically distinct (a−c, $p < 0.01$; d, e, $p < 0.005$).

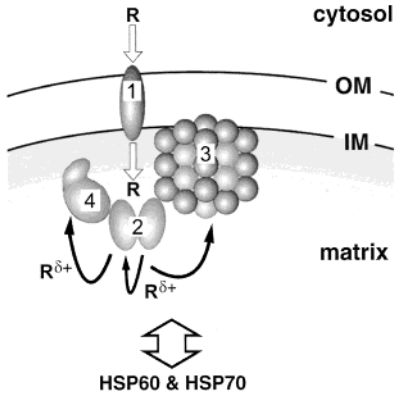


FIGURE 6: Model for events leading to TFEC-mediated cell death in vivo. Transport of the protoxicant TFEC (R) into the mitochondrion by an unidentified transporter (**1**) results in the formation of reactive intermediate (R$^{\delta+}$) and is proposed to be undertaken primarily by native, homodimeric AAT (**2**). AAT-generated R$^{\delta+}$ is removed to other proximal targets, e.g., the αKGDH complex (**3**) and bilobular monomeric aconitase (**4**), by inherent substrate channeling between these components. Secondarily, DFTAL-induced conformational alterations in target proteins signal the recruitment of mitochondrial stress proteins HSP60 and HSP70 for downstream repair processes. The relative positions of the mitochondrial outer membrane (OM), inner membrane (IM), and matrix are indicated.

Only relatively recently have studies begun to address the biochemical mechanism of Fe/S cluster synthesis. Initial work with a bacterial cysteine desulfurase required for nitrogen fixation (NifS) has been expanded to an essential *Saccharomyces cerevisiae* homologue, Nfs1p, also a pyridoxal 5′-phosphate containing C-S lyase with aminotransferase homology (*27*−*29*). In addition, other NifS-related activities in prokaryotes and eukaryotes have been observed. Termed Isc, for *i*ron-sulfur *c*luster assembly, the deletion of these activities usually results in a nonviable phenotype or markedly altered growth properties (*29*, *30*). The remarkable degree of conservation of Fe/S cluster synthesis is highlighted by the recent identification of human Nif homologues (IscS and IscU), suggesting that similar chemistries are likely in various subcompartments of the mammalian cell (*31*, *32*).

From studies such as these, in both prokaryotes and lower eukaryotes, a general role for a L-cysteine-directed desulfurase, with structural homology to AAT (*33*), is apparent in Fe/S cluster formation. In addition, it has been proposed that the inorganic sulfide (S°) so formed can bind to ligand cysteines of aconitase in an intermediate step which precedes mature [4Fe-4S]$^{2+}$ cluster formation (*30*, *33*). If this is also the case in higher eukaryotes, then it would not be unreasonable to suggest that a proximal position for AAT to aconitase would be beneficial in order to minimize cellular damage from general S° release. Although our data are insufficient to directly implicate AAT C-S lyase activity in the generation of S° for de novo aconitase Fe/S cluster synthesis, the close proximity of the two enzymes suggests a role in the maintenance of the aconitase functional state. Nonetheless, further studies (e.g., with in vitro reconstituted systems) will be required to confirm a direct functional interaction between AAT and the maintenance of aconitase Fe/S cluster stability.

Our previous DFTAL adduct localization studies using immunodetection, immunoprecipitation, and radiolabel, in combination with the data presented here, argue for a dynamic interaction between a core metabolic complex (aconitase, AAT, αKGDH) and HSP60/HSP70 within the mammalian mitochondrion (*5*, *6*). From a functional standpoint these data support substrate channeling between AAT and the αKGDH. It is perhaps not surprising that a substrate channeling connection between mitochondrial AAT and αKGDH exists as it can be predicted from common substrate utilization principles alone and has been known for some time (*34*). In addition, however, these data also point to an association between AAT and aconitase which is not immediately intuitive. These associations have been represented in Figure 6 although it cannot be discounted that other components may also form extensions of this higher order complex [e.g., complex I and malate dehydrogenase (*34*, *35*)].

Substrate channeling, i.e., the passage of a common metabolite between two enzymes without equilibrium into the bulk solution, represents a process of microcompartmentation and is of fundamental importance in regulating cellular metabolic pathways (*35*). Compelling evidence in favor of substrate/product channeling between sequential enzymes in metabolic pathways has accumulated but has been limited by the disruptive biochemical procedures usually employed to observe these otherwise weak supramolecular interactions (*35*−*37*). Furthermore, proteins isolated using such physical procedures vary according to the relative

concentration of relevant substrates or products used (*34*). The data presented here complement transdominant inhibition studies in *S. cerevisiae* as information has been obtained with minimal cellular perturbation (*36*).

Other circumstantial evidence for a functional multienzyme complex consisting of aconitase, αKGDH, an aconitase-associated "synthetic" enzyme, and/or mitochondrial stress proteins is evident from cross-linking studies in yeast (*38*) and from the identity of major autoantigens in rheumatic heart disease (*39*). Interestingly, and unexpectedly, deletion of *IscS* in *Escherichia coli* results in an unexplained aerobic thiamin auxotrophy which is reversible in anaerobic conditions (*29*). The two predominant thiamin-requiring enzymes are pyruvate dehydrogenase and αKGDH, the activity of which is known to be lost under anaerobic conditions (*19*). These findings confirm an interdependence between Fe/S cluster synthesis and other non-Fe/S requiring steps of the TCA cycle.

Nine mammalian $\beta$-lyases with activity to cytotoxic cysteine S-conjugates are currently known, yet the activity responsible for TFEC bioactivation remains unknown (*40*). It seems likely, therefore, that the activity responsible for TFEC bioactivation would result in its own covalent modification if accessible lysine residues were available. We have identified all of the DFTAL-modified proteins produced after TFEC dosing in a mammalian model, and mitochondrial AAT is the only protein which satisfies criteria for TFEC metabolism and bioactivation. As a corollary these data explain the otherwise perplexing observations of Cooper and co-workers (*41*), who observed that the presence of α-ketoglutarate markedly increased TFEC-mediated AAT inhibition insomuch as the addition of this substrate would prevent channeling between these two species.

Although we favor the interpretation that these data are indicative of a functional multienzyme interaction on the inner mitochondrial membrane between AAT, αKGDH, and aconitase, other equally plausible explanations are also possible. For example, these DFTAL-labeled proteins may share a common physiochemical attribute, e.g., particularly nucleophilic and accessible lysine residues, which render them more susceptible to modification. Alternatively, AAT, αKGDH, and aconitase may simply represent species in very high abundance adjacent to the site of reactive intermediate formation, and other lower abundance, but similarly modified, proteins have not yet been identified. The further mass spectral characterizations of adducted lysine residues in such DFTAL-modified proteins will help to clarify this issue.

In conclusion, we report here the identification of the final major mitochondrial protein modified during TFEC-induced tissue damage, thereby expanding the list of known DFTAF targets from mitochondrial stress proteins (HSP60 and HSP70) and the α-ketoglutarate dehydrogenase subunits lipoamide succinyltransferase and dihydrolipoamide dehydrogenase. Both in vivo and in vitro mitochondrial aconitase activities were also substantially decreased soon after dosing with TFEC and as a consequence of DFTAL modification. The in situ labeling characteristics of bioactivated TFEC have additionally provided information regarding the likelihood of substrate channeling between AAT and αKGDH as well as revealing a close physical association between AAT and aconitase. Moreover, the desulfurase activity associated with AAT suggests that AAT may be required for the maintenance of aconitase activity in situ. As such, AAT can be considered to have a bifunctional role in the maintenance of TCA cycle activity. We further propose that the desulfurase activity of mitochondrial AAT is the biologically relevant $\beta$-lyase (C-S lyase) activity responsible for TFEC bioactivation and cell death.

## ACKNOWLEDGMENT

We thank Dr. Lance Pohl (NIH) for the generous gift of DFTAL-specific antibody, Drs. M. W. Anders (University of Rochester) and A. J. L. Cooper (Weill Medical College of Cornell University) for helpful advice, and Cathy Yeung for assistance with aconitase enzyme assays. The expert assistance of Karen L. de Mesy Jensen and the Electron Microscopy Research Core at the University of Rochester is also appreciated.

## REFERENCES

1. Nelson, S. D., and Pearson, P. G. (1990) *Annu. Rev. Pharmacol. Toxicol. 30*, 169−195.
2. Pumford, N. R., and Halmes, N. C. (1997) *Annu. Rev. Pharmacol. Toxicol. 37*, 91−117.
3. Prescott, L. F. (1996) *Paracetamol (acetaminophen): a critical bibliographic review*, Taylor and Francis, London.
4. Pohl, L. R. (1993) *Chem. Res. Toxicol. 6*, 786−793.
5. Bruschi, S. A., Lindsay, J. G., and Crabb, J. W. (1998) *Proc. Natl. Acad. Sci. U.S.A. 95*, 13413−13418.
6. Bruschi, S. A., West, K. A., Crabb, J. W., Gupta, R. S., and Stevens, J. L. (1993) *J. Biol. Chem. 268*, 23157−23161.
7. Anders, M. W., and Dekant, W. (1998) *Annu. Rev. Pharmacol. Toxicol. 38*, 501−537.
8. Shevchenko, A., Wilm, M., Vorm, O., and Mann, M. (1996) *Anal. Chem. 68*, 850−858.
9. Yates, J. R., III, Carmack, E., Hays, L., Link, A. J., and Eng, J. K. (1999) *Methods Mol. Biol. 112*, 553−569.
10. Gygi, S. P., Rochon, Y., Franza, B. R., and Aebersold, R. (1999) *Mol. Cell. Biol. 19*, 1720−1730.
11. Eng, J. K., McCormack, A. L., and Yates, J. R., III (1994) *J. Am. Soc. Mass Spectrosc. 5*, 976−989.
12. Yates, J. R., III, Eng, J. K., McCormack, A. L., and Schieltz, D. (1995) *Anal. Chem. 67*, 1426−1436.
13. Wu, J. C., Merlino, G., Cveklova, K., Mosinger, B., Jr., and Fausto, N. (1994) *Cancer Res. 54*, 5964−5973.
14. Andersson, U., Leighton, B., Young, M. E., Blomstrand, E., and Newsholme, E. A. (1998) *Biochem. Biophys. Res. Commun. 249*, 512−516.
15. Das, N., Levine, R. L., Orr, W. C., and Sohal, R. S. (2001) *Biochem. J. 360*, 209−216.
16. Cabiscol, E., Piulats, E., Echave, P., Herrero, E., and Ros, J. (2000) *J. Biol. Chem. 275*, 27393−27398.
17. Hausladen, A., and Fridovich, I. (1994) *J. Biol. Chem. 269*, 29405−29408.
18. Castro, L. A., Robalinho, R. L., Cayota, A., Meneghini, R., and Radi, R. (1998) *Arch. Biochem. Biophys. 359*, 215−224.
19. Haller, R. G., Henriksson, K. G., Jorfeldt, L., Hultman, E., Wibom, R., Sahlin, K., Areskog, N. H., Gunder, M., Ayyad, K., Blomqvist, C. G., et al. (1991) *J. Clin. Invest. 88*, 1197−1206.
20. Rotig, A., de Lonlay, P., Chretien, D., Foury, F., Koenig, M., Sidi, D., Munnich, A., and Rustin, P. (1997) *Nat. Genet. 17*, 215−217.
21. Groves, C. E., Lock, E. A., and Schnellmann, R. G. (1991) *Toxicol. Appl. Pharmacol. 107*, 54−62.
22. Zou, S., Meadows, S., Sharp, L., Jan, L. Y., and Jan, Y. N. (2000) *Proc. Natl. Acad. Sci. U.S.A. 97*, 13726−13731.
23. Fiore, C., Trezeguet, V., Le Saux, A., Roux, P., Schwimmer, C., Dianoux, A. C., Noel, F., Lauquin, G. J., Brandolin, G., and Vignais, P. V. (1998) *Biochimie 80*, 137−150.
24. Commandeur, J. N., De Kanter, F. J., and Vermeulen, N. P. (1989) *Mol. Pharmacol. 36*, 654−663.

25. Commandeur, J. N., and Vermeulen, N. P. (1990) *Chem. Res. Toxicol. 3*, 171−194.
26. Talbot, R. J. E. (1972) *Compr. Chem.Kinet. 10*, 209−293.
27. Li, J., Kogan, M., Knight, S. A., Pain, D., and Dancis, A. (1999) *J. Biol. Chem. 274*, 33025−33034.
28. Strain, J., Lorenz, C. R., Bode, J., Garland, S., Smolen, G. A., Ta, D. T., Vickery, L. E., and Culotta, V. C. (1998) *J. Biol. Chem. 273*, 31138−31144.
29. Schwartz, C. J., Djaman, O., Imlay, J. A., and Kiley, P. J. (2000) *Proc. Natl. Acad. Sci. U.S.A. 97*, 9009−9014.
30. Zheng, L., Cash, V. L., Flint, D. H., and Dean, D. R. (1998) *J. Biol. Chem. 273*, 13264−13272.
31. Tong, W. H., and Rouault, T. (2000) *EMBO J. 19*, 5692−5700.
32. Land, T., and Rouault, T. A. (1998) *Mol. Cell 2*, 807−815.
33. Clausen, T., Kaiser, J. T., Steegborn, C., Huber, R., and Kessler, D. (2000) *Proc. Natl. Acad. Sci. U.S.A. 97*, 3856−3861.
34. Fahien, L. A., Kmiotek, E. H., MacDonald, M. J., Fibich, B., and Mandic, M. (1988) *J. Biol. Chem. 263*, 10687−10697.
35. Srere, P. A. (1987) *Annu. Rev. Biochem. 56*, 89−124.
36. Velot, C., and Srere, P. A. (2000) *J. Biol. Chem. 275*, 12926−12933.
37. Schagger, H., and Pfeiffer, K. (2000) *EMBO J. 19*, 1777−1783.
38. Kaufman, B. A., Newman, S. M., Hallberg, R. L., Slaughter, C. A., Perlman, P. S., and Butow, R. A. (2000) *Proc. Natl. Acad. Sci. U.S.A. 97*, 7772−7777.
39. Tontsch, D., Pankuweit, S., and Maisch, B. (2000) *Clin. Exp. Immunol. 121*, 270−274.
40. Cooper, A. J., Bruschi, S. A., and Anders, M. W. (2002) *Biochem. Pharmacol.* (in press).
41. Kato, Y., Asano, Y., and Cooper, A. J. (1996) *Dev. Neurosci. 18*, 505−514.

BI020038J